

## Numerical modelling of three-dimensional fatigue crack closure: plastic wake simulation

D. Camas, J. Garcia-Manrique<sup>1</sup>, F. Perez-Garcia, A. Gonzalez-Herrera

Departamento de Ingeniería Civil, de Materiales y Fabricación, Universidad de Málaga,

Escuela de Ingenierías Industriales, C/ Doctor Ortiz Ramos, s/n.

Campus de Teatinos, E-29071, Málaga, Spain

Phone +34 951952440;

[josegmo@uma.es](mailto:josegmo@uma.es)

### Abstract

Finite element method has been broadly used to study fatigue crack closure. The simulated plastic wake length is one of the key modelling parameters involved. This paper presents a complete analysis in fatigue crack closure 3-D models.

It is aimed at two aspects: the influence on the calculation of opening and closure values, and the effect on other main results. Conclusion indicates a 0.6· times Dugdale's plastic size length to stabilise results as plastic zone or contact area, but a reduced length could be acceptable in terms of crack closure results. This suggests some independence among this parameter and fatigue crack closure.

**Keywords:** finite element analysis, fatigue crack closure, plastic wake, crack growth.

## Nomenclature

a	Crack length
b	Specimen thickness
$K_{max}$	Maximum stress intensity factor
$K_{min}$	Minimum stress intensity factor
$K_{ttop}$	Crack opening, tip tensile criterion
$K_{ttcl}$	Crack closure, tip tensile criterion
$K_{ncop}$	Crack opening, node contact criterion
$K_{ncccl}$	Crack closure, node contact criterion
R	Stress ratio
$r_{pD}$	Dugdale's Plastic zone size
$s_{me}$	Minimum element size in the crack tip
$\Delta a_i$	Crack advance length per cycle
$\Delta a_w$	Simulated plastic wake
$\eta$	Number of divisions of the plastic zone

## 1. INTRODUCTION

In the last decades, the interest of the study of the Plasticity Induced Crack Closure (PICC) phenomenon is unquestionable. Elber [1] introduced this concept and the effective range of crack growth were narrowed in terms of the nature of the contact between the faces of the crack. Since then, much progress has been made in the analysis of the closure mechanisms (Ritchie and Suresh [2,3]) and different formulations have been proposed to include these considerations within an effective range of the stress intensity factor with which to modify the well-known Paris' law.

In many ductile materials, with strong plasticity behaviour, subjected to cyclic loads, it is considered that the PICC has a great influence on the rate of crack growth and it could become the driving force thereof. During the growth of the crack, the plasticised areas on the crack front generate a volume of residual yielding material known as plastic wake. This plasticized material produces a premature contact between the edges of the crack that delays its rate of growth. The PICC study therefore focuses on identifying this effective range of crack growth.

PICC experimental research is complex. The presented results show great deviations between some authors and others (Ashbaugh [4] – Ray [5]). Yisheng and Schijve [6] suggest that the spread inherent to the methods is of the order of 15%. Other more current techniques, such as digital imaging correlation, presents more accuracy in recent fatigue crack growth studies [7–9]. However, with this technique only data on the surface is available, but maintain the impossibility of observing the interior of the specimen.

Therefore, the numerical simulation soon became a tool of great value in this field. However, it has been a complicated process to develop a work scheme that gives certainty to the results, since the experimental validation is not possible in many cases. This has been one of the main research lines of the authors of this article. From the beginning, the great variety of parameters, both physical and purely numerical that

1 were interrelated, was identified [10–12]. It was necessary to analyse them separately and establish robust  
2 methodologies where the influence of each one on the convergence of crack closure results was clearly  
3 established. On the one hand, the influence of the thickness, the load level and the curvature on the  
4 yielded areas were studied [13,14] under homogenous distributions of the stress intensity factor (K) along  
5 the crack front. On the other hand, the actual three-dimensional effect of the distribution of K on the  
6 crack front was analysed [15,16]. In a recent work [17], both lines of research were unified and a  
7 corrected methodology to evaluate plasticity induced crack closure was presented. In addition, it was  
8 concluded that numerical-experimental correlations can be improved taking advantage of the pivot node  
9 area [18].

10  
11  
12  
13  
14 The numerical simulations were carried out using the finite element method. They are complex non-linear  
15 problems where the numerical parameters must be adjusted in a coordinated way. The analysis of  
16 convergence towards stable results must always be part of the calculation process. Parameters such as the  
17 simulation methodology of the contact between the faces, the type of elements or the mesh distribution,  
18 have a great influence on the results and the numerical convergence of the solution. In the early stages of  
19 this research, one of the main difficulties encountered was the few bibliographic references in this regard.  
20 Even, the lack of justification of these parameters in numerous works.

21  
22  
23  
24  
25 In 2009, Gonzalez-Herrera and Zapatero[19] presented a very interesting work on this topic applied to the  
26 bidimensional case. In this study, both numerical relationships and the physical implications of the  
27 relationship between the opening and closure results and the history of previous loads were presented.  
28 Recommendations were offered for plane stress and plane strain according to the stress ratio R. However,  
29 nowadays the new computational capabilities make that the majority of numerical simulations already  
30 approach the subject from a three-dimensional perspective. It can be found several lines of research that  
31 involve a previous process of crack growth and where the plastic wake can affect the convergence of the  
32 results.  
33

34  
35  
36  
37  
38 In 2007, Alizadeh et al. [20] have already compared two and three-dimensional analyses of fatigue crack  
39 closure with good agreement between three-dimensional results at the surface and bi-dimensional plane  
40 stress ones. The 3-D mid-plane and the plane strain results, presented this agreement only for large  
41 thicknesses.  
42

43  
44  
45 In 2016, Gardin et al. presented two works where this crack growth was simulated in CT specimens of  
46 304L stainless steel: on the one hand [21], addressing the prediction of crack front shape during fatigue  
47 propagation and, on the other hand [22], expanding numerical simulation of PICC to curved crack shapes.  
48 In the first of them, the crack propagations extended until the stabilization of the crack front shape with a  
49 total length of 3mm for the analysed model. In the second one, the length of the crack oscillated from  
50 0.1mm to 1.5mm, based on the previous recommendations by Vor et al. [23]. In this study, the specific  
51 case of this material was analysed for a  $\Delta K$  of 12 MPa·m<sup>1/2</sup> and R=0.1. There are many other authors,  
52 who also generate a plastic wake in their contributions, as Antunes et al. [24] that studies the effect of  
53 compressive loads on PICC, or Borrego et al. [25] who analyse the influence of overloads.  
54  
55  
56  
57  
58  
59  
60  
61  
62  
63  
64  
65

1  
2 There is no consensus regarding the parameter that determines crack opening or closure instant during  
3 each fatigue cycle. The literature presents two clearly defined trends for determining crack opening. The  
4 first considers that the crack opens when there is no physical contact between the free surfaces (Knc). The  
5 second tendency studies the stresses perpendicular to the plane of the crack at the crack tip (Ktt). This  
6 paper does not present enough data to compare both methods. What it intends is to establish the wake  
7 length necessary to be able to ensure that the results obtained numerically have converged. In our opinion,  
8 it is necessary to continue improving the opening and closing calculation methodology. In a recent work,  
9 we propose some recommendations on the subject [17]. However, we must also consider the effect of  
10 other phenomena, such as the vertex singularity, that affect the region near the surface and are not  
11 included here.

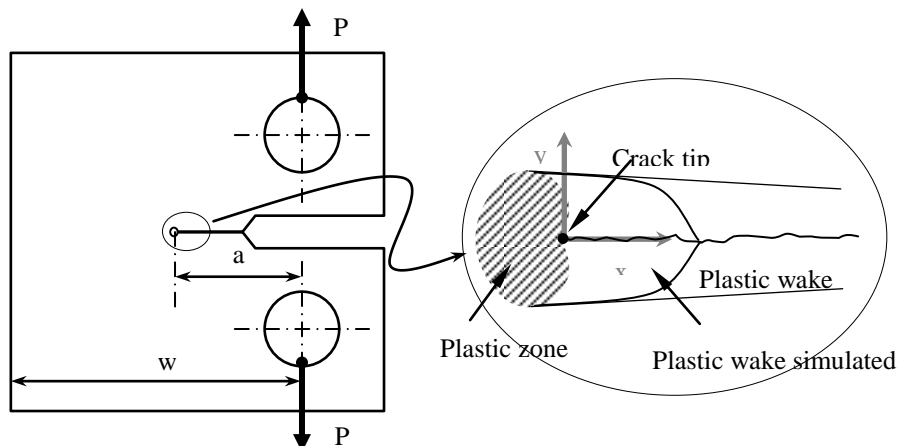
12  
13  
14  
15  
16  
17 In a recent contribution, Camas et al. [26] already presented recommendations on mesh refinement for the  
18 numerical modelling of three-dimensional fatigue crack closure. Mesh recommendations and minimum  
19 element size were presented around the crack front.

20  
21  
22  
23 In this paper, another fundamental parameter when numerically simulating a fatigue crack growth process  
24 is studied, the plastic wake length. Therefore, the aim of this work is to analyse, three-dimensionally, the  
25 influence of the plastic wake length on the accuracy of parameters related with PICC. The numerical  
26 accuracy is analysed in terms of crack closure and opening values along the specimen thickness, and in  
27 terms of stress and strain fields.

28  
29  
30  
31 In the following sections, the analysis methodology is briefly described; it is based on references and  
32 completed with the experience of the present authors. The influence of the plastic wake simulated on the  
33 crack opening and closure values is presented in section 3. This is completed with the analysis of the  
34 plastic zone and the contact area in section 4. Finally, the main recommendations are outlined in the  
35 conclusions.

## 36 37 38 39 **2. FINITE ELEMENT MODELLING**

40  
41 The main issues regarding the Finite Element modelling methodology will be briefly described in this  
42 section. There is a set of key parameters affecting the modelling process that must be carefully selected.  
43 The meshing and the element size, the material behaviour model, the loading cycles and crack growth  
44 scheme, the contact simulation, the plastic wake and the opening and closure definition are issues which  
45 will be discussed succinctly. There are many other references dealing with specific details [12,26]. This  
46 methodology has been developed by the authors based in the literature and their own experience.



1  
2  
3  
4 **Fig. 1.** CT specimen description  
5

6 A three-dimensionally model of a CT specimen has been modelled for this study. The commercial finite  
7 element (FE) software ANSYS has been employed. Fig. 1 shows a scheme with the main dimensions,  
8 where  $a$  is the crack length and  $b$  the specimen thickness. A 3 mm specimen thickness has been  
9 considered, being  $W = 50$  mm and  $a = 20$  mm the other characteristic dimensions. The load applied in this  
10 study is that corresponding to a stress intensity factor  $K_{max}=25$  MPa·m<sup>1/2</sup> and simulations are carried out  
11 considering  $R=0.1, 0.3$  and  $0.7$ .  
12  
13  
14

15  
16 This combination of small thickness and high load level, provides a case where transition along the  
17 thickness is significant for the main results (as the plastic zone [27]), being very representative with  
18 limited computational costs.  
19

20  
21 The material used is an Al-2024-T351 aluminium alloy that shows weak hardening ( $E=73.5$ GPa,  
22  $\sigma_{yield}=425$ MPa,  $K'=685$ MPa,  $n'=0.073$ , being  $K'$  and  $n'$  the parameter and the exponent in the Ramberg-  
23 Osgood yielding model). It has been modelled with an isotropic hardening rule (with  $H/E=0.003$ ) using a  
24 bi-linear diagram to define the stress-strain curve.  
25  
26

27  
28 The conclusions of this paper are limited to materials with small hardening as the considered in this study  
29 (those with  $H/E<0.03$ ). For these materials, an isotropic or a kinematic hardening rule can be considered  
30 indistinctively. The convergence of the results is independent of the specific hardening rule considered.  
31

32  
33 Different material properties as for example different yield stresses are not affecting the  
34 recommendations. These are related to the Dugadale's plastic size, which depends on the yield stress. The  
35 yielding areas can be smaller or bigger without any problem because the minimum element size and the  
36 plastic wake length is going to be affected by this parameter. However, it is important to highlight that  
37 other materials with bigger hardening values requires a deeper analysis to reach a valid conclusion.  
38 However, this is out of the scope of the present work.  
39  
40  
41

## 42 **2.1 General issues**

43  
44 Fig.2 shows the FE model. Due to the double symmetry, only a quarter of the specimen must be  
45 represented. In order to obtain proper results, the volume surrounding the crack tip is the most critical.  
46 Huge gradients in the stress and strain fields are present and must be properly captured. This makes  
47 necessary that the size of the elements around the crack tip must be small enough. However, to limit the  
48 computational cost, a huge transition from this zone to the most remote ones must be arranged. To  
49 accomplish this, the specimen has been divided in two different volumes. In the first one, around the  
50 crack front, a homogeneous and uniform structured mesh with hexahedral elements is made. In the second  
51 one, the material will be in elastic range during the whole loading process and so it can be meshed with  
52 tetrahedral elements, allowing a smooth transition. The homogeneous region around the crack front and  
53 the transition one can be seen in Fig.2.  
54  
55  
56  
57  
58  
59  
60  
61  
62  
63  
64  
65

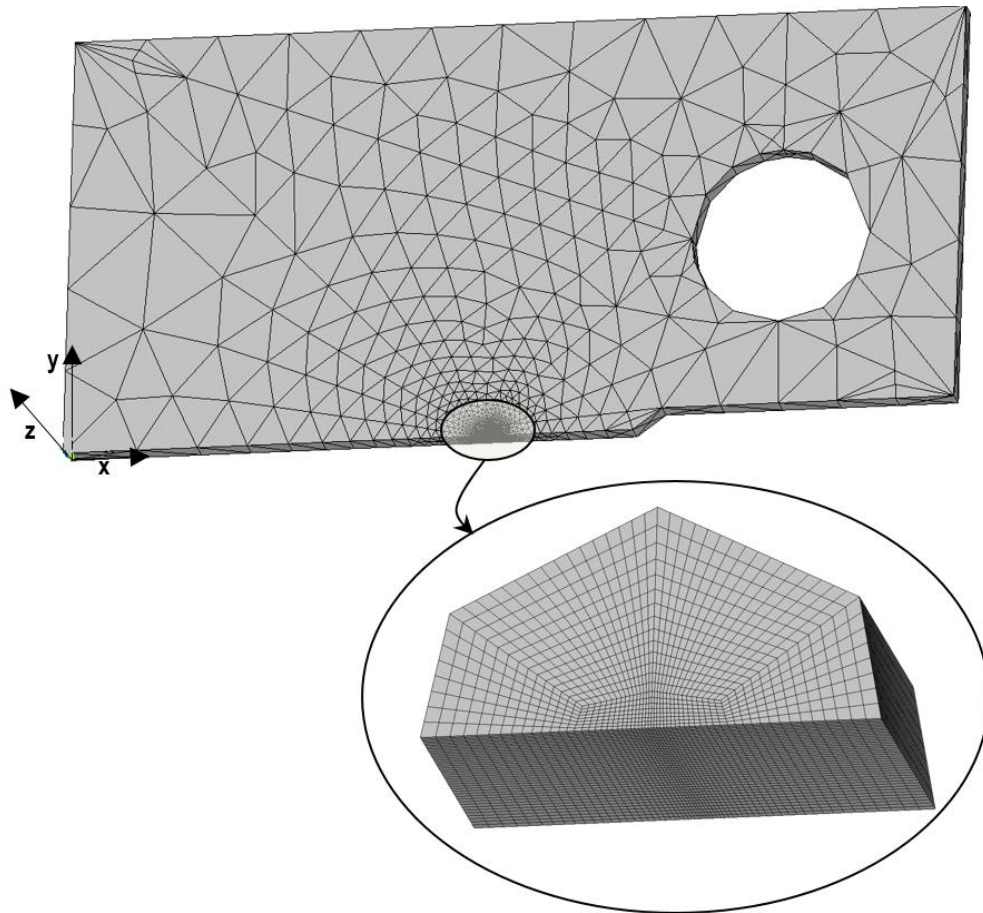


**Fig. 2.** 3D finite element model

To model the vicinity of the crack tip, there is a general agreement on the use of a regular mesh with linear or quadratic square (2D) or hexahedral (3D) elements. However, following the methodology developed in 2D studies (Gonzalez-Herrera and Zapatero [19]), a mesh size transition reduction is used. Elements closer to the crack tip are the smaller and their size grow as they separate from that point (see schematically in Fig.3).

As the mesh size requirements are related to the size of the elements at the crack tip, this strategy provided two advantages to decrease the computational cost. On the one hand the model has fewer elements and, on the other hand, the number of load cycles necessary to develop the plastic wake is lower. It was proved that with a mesh transition lesser than a 15% reduction of the elements sizes, the results do not suffer any significant variation. This is of particular interest for the present study where the influence of the plastic wake is studied. For this model, the transition rate has been taken into consideration as an upper limit, allowing only transitions with lower rates than 8% far from the crack front and 4% near the final crack front.

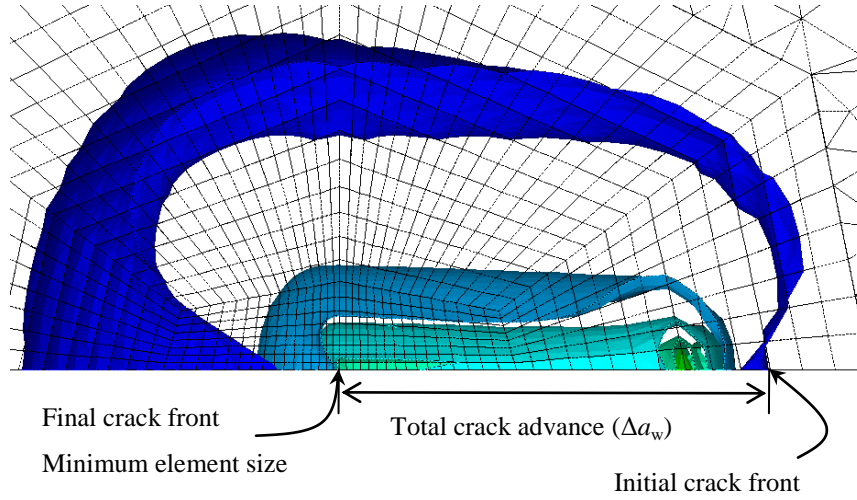


**Fig. 3.** Total crack growth to develop the plastic wake. Progressive mesh scheme

The minimum element size considered for all the cases analysed in this study is  $\eta=90$ , being above the recommendation obtained in a previous study [26]. This is one of the most influential parameters in these simulations and has been widely studied in 2D and 3D works. It is defined by a dimensionless term:

$$\eta = r_{pD} / s_{me} \quad (1)$$

where  $r_{pD}$  is the plastic zone size according to Dugdale's equation (Eq. 2) and  $s_{me}$  is the size of the element at the crack tip (minimum element size). This parameter represents the number of divisions in which the plastic zone would be meshed whether a regular lattice of elements equal to the smallest one had been used. So  $\eta=90$  is a length 90 times smaller than the Dugdale's plastic size ( $r_{pD}$ ).

$$r_{pD} = \frac{\pi}{8\alpha} \left( \frac{K_I}{\sigma_y} \right)^2 \quad (2)$$

In the Dugdale's expression (Eq. 2),  $\alpha$  is a constraint factor equal to 1 for plane stress and 3 for plane strain. As in this work, a 3D model is considered,  $\alpha$  has been taken equal to 1 in order to be higher than any yielded zone size along the thickness. All the results and parameters will be referred to this value in plane stress ( $\alpha=1$ ). The working methodology does not consider the behavior to be comparable to plane stress. The  $r_{pD}$  parameter here is used as a reference to establish a fine mesh zone around the crack front. For the entire thickness of the specimen. This way we achieve that, for each load case, the mesh density is adequate.

Regarding the mesh size along the thickness, according to previous studies [14,27,28], results close to the mid plane, where plane strain conditions are dominant, are quite constant, while when approaching the external surface of the specimen, there is an important transition on the strain and stress fields. In order to capture properly this transition without consuming computational cost, the length along the thickness of the elements next to the surface is half the length of the elements next to the mid plane of the specimen. Outside this region, the number of through-thickness divisions was strongly reduced to speed up the calculations.

1 The crack growth scheme is another key aspect. Computing all the cycles involved in a real fatigue crack  
2 growth process is not affordable from a computational point of view. So the crack growth is modelled by  
3 means of a limited number of cycles, changing the boundary condition from one cycle to the next to  
4 simulate the crack advance. This implies an artificial process that must be carefully designed to avoid  
5 computational errors. A balance between mesh size, plastic wake length developed and the number of  
6 applied cycles must be found.  
7

8  
9 Fig. 3 shows the progressive mesh scheme considered and the final plastic wake developed. The coloured  
10 regions represents different equivalent plastic strains assumptions. The outer boundary, the navy-blue  
11 contour, comprehend the whole yielded volume, while the rest regions correspond to different plastic  
12 strain levels which are higher the smaller the contours are. The figure is a lateral view of the yielded  
13 volume. These are represented to show qualitatively the evolution of the strain. It can be seen that,  
14 although the evolution of the outer boundary is smooth, there is a change in the behaviour for the higher  
15 strain levels. That is the reason why it is necessary to develop a certain plastic wake to be far away from  
16 the beginning of the crack growth to stabilise the results.  
17

18  
19 Crack growth is carried out changing the boundary conditions. In this work, a node is released at each  
20 load cycle in order to obtain a strain field as continuous as possible. There is some controversy regarding  
21 the most appropriate moment to release the nodes, nevertheless the most accepted criterion is to release  
22 nodes at maximum load [11,29–32]. This is the criterion that has been followed in the present study. It  
23 has a great physical sense and there are lesser possibilities of numerical instabilities.  
24

25  
26 The other key point regarding the crack growth scheme is the number of load cycles simulated between  
27 node releases. In three-dimensional analysis usually only one load cycle is applied because of the  
28 numerical cost [7, 16, 27]. Considering the low hardening rate for this material, it has proved to be valid.  
29 In order to facilitate the convergence during the first steps of crack growth, first loading cycles are  
30 applied increasing gradually their values without allowing the crack growth, until the maximum load is  
31 achieved.  
32

33  
34 Finally, regarding crack opening and closure definition, the two different criteria widely used in the  
35 bibliography [33,34] are employed. The first one is based on the displacements of the first node behind  
36 the crack front (node contact criterion), while the second one is based on the stresses at the crack front  
37 (tip tension criterion).  
38

39  
40 The node contact criterion defines the opening when the first node behind the crack front loses contact  
41 with the target surface and is denoted with the subscript *nc*. The other criterion, based on the stresses,  
42 defines the opening when the stress at the node located at the crack front turns from compression to  
43 tension. This criterion is denoted as tip tension and is represented with the subscript *tt*. Crack opening is  
44 denoted with the subscript *op* and closure as *cl*. Thus,  $K_{ncop}$  and  $K_{ttop}$  represent the opening values  
45 determined by the node contact and the tip tension criteria respectively, while  $K_{nccl}$  and  $K_{ttcl}$ , the closure  
46 ones.  
47

## 48 **2.2 Plastic wake**

49  
50  
51  
52  
53  
54  
55  
56  
57

The minimum plastic wake length ( $\Delta a_w$ ) that is necessary to compute is a critical parameter because it influences strongly the results. In the bibliography, two different main ways of analysing the minimum crack length can be found. The first one [8, 29, 30] consists in analysing the opening/closure values when increasing the crack length until a stabilised value is obtained. But for this option, a regular lattice mesh is necessary, which is not the case in the present study. In the other one [3], the final crack length is equal for all the different plastic wake lengths analysed and the difference is that the initial crack front is placed at different distances (as is outlined in Fig.3).

This approach presents a series of advantages. One of them is that the final results are always obtained at the same position, with the same mesh, so no meshing errors may affect to the results. The others are in terms of computational cost reduction. As the final data from last cycle is the only relevant information to be processed, less data must be stored. Moreover, a more efficient mesh is allowed reducing strongly the computational cost but remaining the same accuracy. As described in the previous subsection, a transitory mesh towards the crack tip decreases the number of elements and the number of cycles to be simulated.

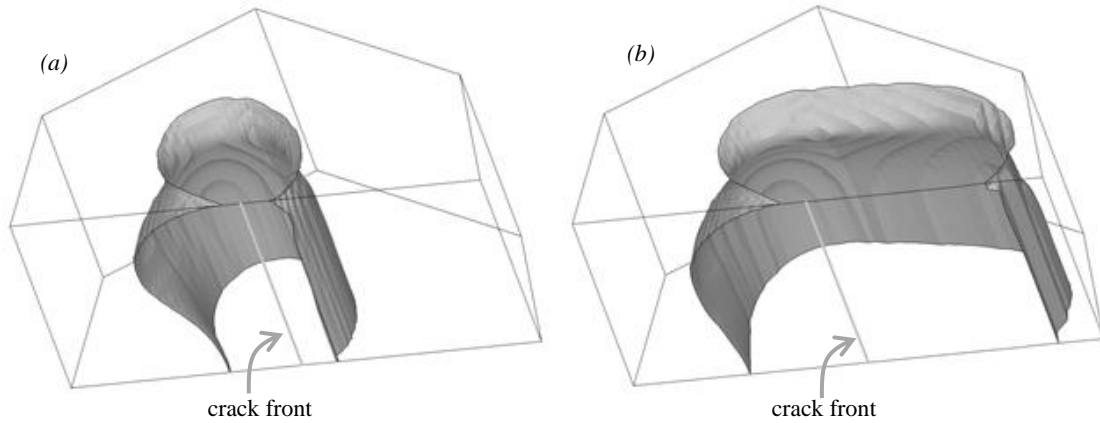


**Fig. 4.** Plastic wake starting at different initial crack fronts. (a)  $\Delta a=0.05 \cdot r_{pD}$ . (b)  $\Delta a=0.6 \cdot r_{pD}$

The main disadvantage is that the lengths of the plastic wake necessary to obtain valid result must be established previously in order to determine the initial point of the crack. As mentioned before, previous bi-dimensional work which analysed the plastic wake length influence on plane strain and stress conditions [19] was done. Due to the computational cost of these studies in the 3D case, 2D conclusions were extended to the wake simulation on 3D problem. The present work completes these studies for 3D case.

A series of calculations were performed for three different values of R: R=0.1, 0.3 and 0.7. For each case, up to six different plastic wake length (defined as  $\Delta a_w / r_{pD}$ ) values were simulated ranging from 0.05 to 0.8 (0.05, 0.1, 0.2, 0.4, 0.6 and 0.8). Additional control calculations were made to assure that the element size or other parameters were not influencing the results and the main conclusions of the study. It must be remarked the time consuming of each simulation which varies, for the same computer configuration (i7 with 8Gb), from 55 hours of the  $0.8 \cdot r_{pD}$  case to the 5 hours of the  $0.05 \cdot r_{pD}$  one. These times correspond to the R=0.1 case.

### 3. Crack opening and closure

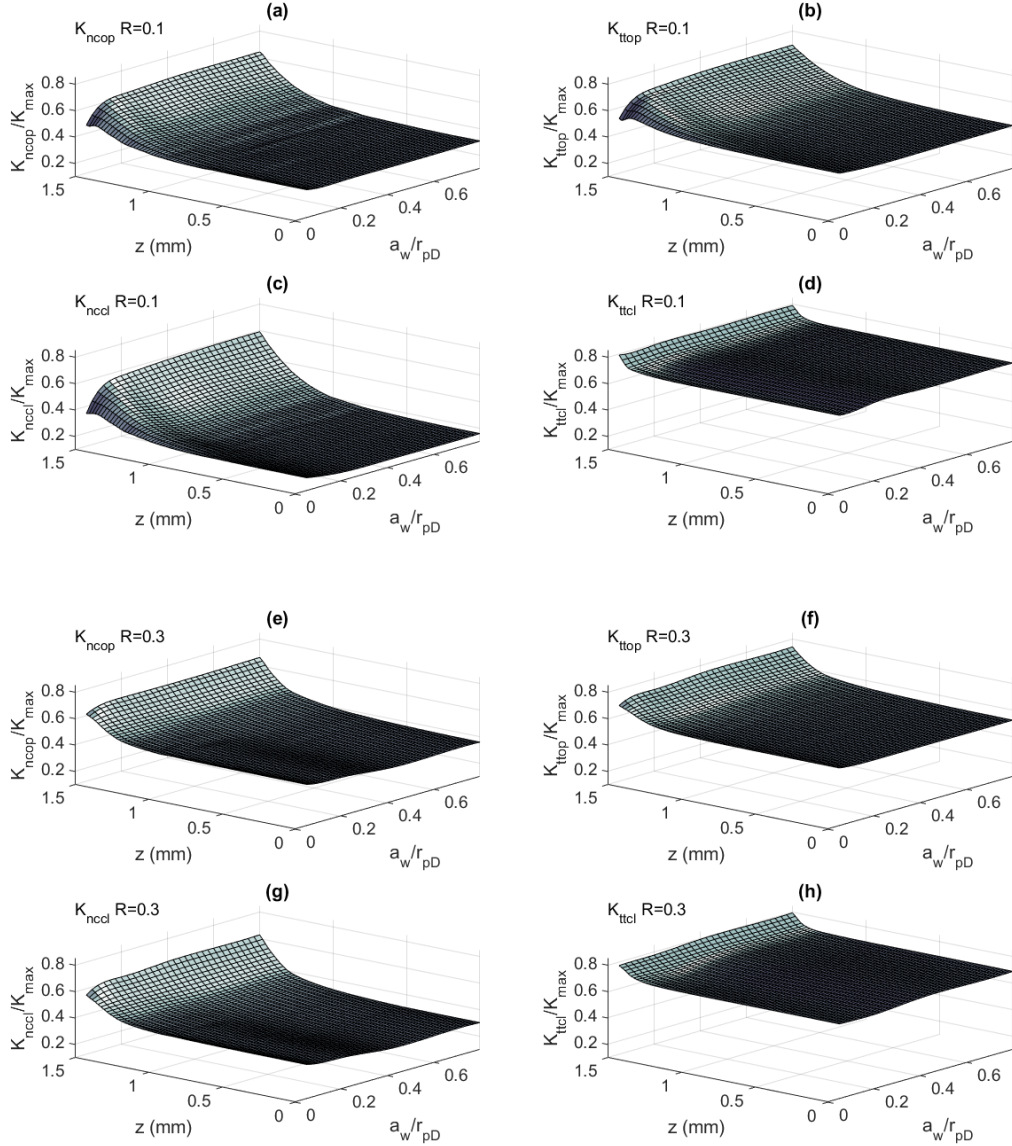


**Fig. 5.** Crack opening and closure values along the thickness in terms of the plastic wake length simulated with different criteria. (a)  $R=0.1$   $K_{ncop}$  (b)  $R=0.1$   $K_{ttop}$  (c)  $R=0.1$   $K_{nccl}$  (d)  $R=0.1$   $K_{ttcl}$  (e)  $R=0.3$   $K_{ncop}$  (f)  $R=0.3$   $K_{ttop}$  (g)  $R=0.3$   $K_{nccl}$  (h)  $R=0.3$   $K_{ttcl}$

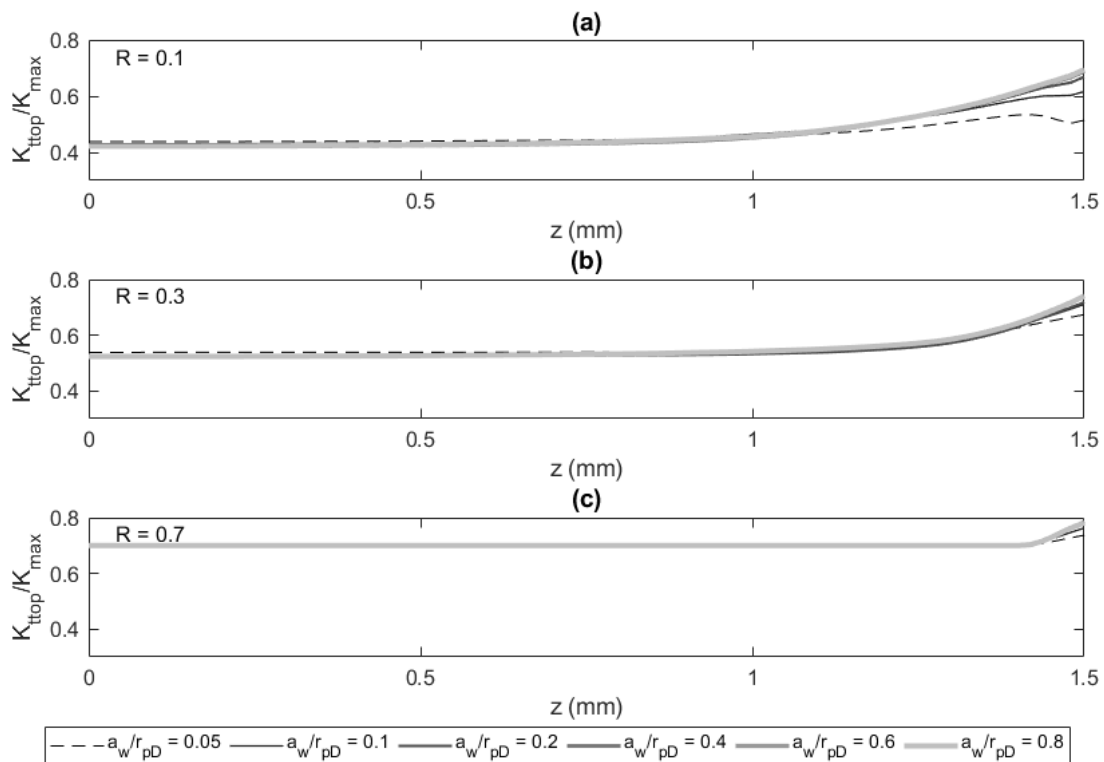
Previous bi-dimensional studies provided an exponential relation between the plastic wake simulated and the opening and closure values [23] in plane stress. The necessary plastic wake simulated ranged from one  $r_{pD}$  for  $R=0$  to  $0.05 \cdot r_{pD}$  for  $R=0.7$ . Plane strain results proved that a  $0.1 \cdot r_{pD}$  plastic wake must be calculated regardless of  $R$ . Given that in 3D calculation both conditions were present, the more constraining case was plane stress.

Fig.5 summarizes the results obtained for  $R=0.1$  and  $R=0.3$ . Both crack opening and closure values with the two different criteria used are shown. These values are presented along the thickness ( $z$  scale,  $z=0$  is the middle plane and  $z=1.5$  mm correspond to the surface) for the different calculations made for each

value of  $\Delta a_w / r_{pD}$ . Take into account that, due to the methodology employed, each result along the thickness is the final result, at the same crack tip but starting at different crack fronts according to the plastic wake simulated (see Fig.4). A continuous graph has been plotted in order to visualize the trend of the influence of  $\Delta a_w / r_{pD}$ . Results for  $R=0.7$  are not plotted due to the negligible influence of the plastic wake. It will be commented later.

The general trend that can be observed in these results is a limited influence of the plastic wake even at the lower value of  $R$ . At the interior of the specimen ( $z=0$ ), the influence seems to be negligible. At the exterior, an exponential effect similar to the results obtained with plane stress is shown. The plastic wake has no effect on  $K_{tcl}$  criteria (Fig.5d and Fig.5h) in accordance with previous observation of the significance of this criteria. Opening and  $K_{ncl}$  presents similar tendencies.

Fig.6 shows the crack opening tip tension ( $K_{ttop}$ ) values along the thickness ( $z$  scale,  $z=0$  is the middle plane and  $z=1.5$  mm correspond to the surface) calculated with different plastic wake lengths for  $R=0.1$ ,  $0.3$  and  $0.7$ . At first sight, it can be observed that the results are quite similar for plastic wake lengths greater than  $0.2 \cdot r_{pD}$  for  $R=0.1$  and at  $0.1 \cdot r_{pD}$  for  $R=0.3$  and  $R=0.7$ . The values along the thickness basically collapse in a single curve for higher plastic wakes making unnecessary the computational cost of its simulation. For the case  $R=0.7$ , this is the only influence of the wake as the other criterion do not show any opening or closure presence. In general, these results are less demanding than those observed in bidimensional studies where, for instance, for  $R=0.1$  a plastic wake above  $0.5 \cdot r_{pD}$  should be calculated [19].



**Fig. 6.**  $K_{ttop}/K_{max}$  evolution with the plastic wake length,  $R=0.1$  (a),  $R=0.3$  (b) and  $R=0.7$  (c)

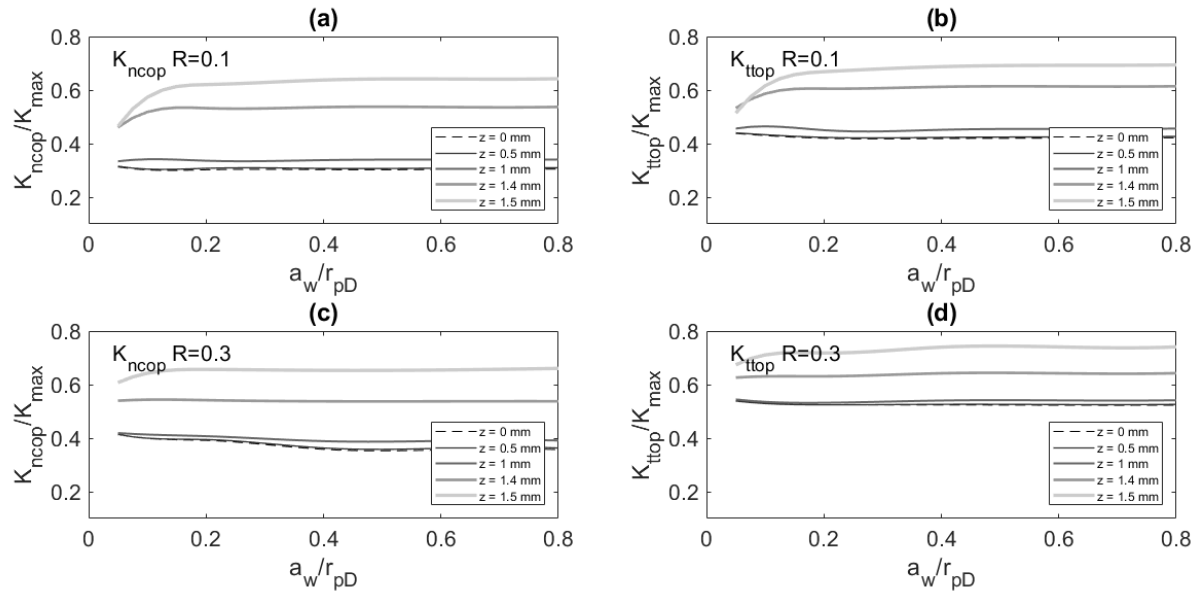


**Fig. 7.** Evolution with the plastic wake length for different planes along the thickness (a)  $R=0.1$   $K_{ttop}/K_{max}$  (b)  $R=0.1$   $K_{ncop}/K_{max}$  (c)  $R=0.3$   $K_{ttop}/K_{max}$  (d)  $R=0.3$   $K_{ncop}/K_{max}$

In order to clarify and to analyse how is the evolution along the thickness, Fig.7 shows the opening results ( $K_{ttop}$  and  $K_{ncop}$ ) at different planes along the thickness ( $z=0, 0.5, 1, 1.4$  and  $1.5$  mm) for  $R=0.1$  and  $R=0.3$ . As the results vary mainly in the first 0.5 mm close to the surface, three different planes have been considered within these distance including results obtained at 0.1 mm from the exterior face. As usual,  $z=1.5$  mm represents the values at the surface, while  $z=0$ , the ones at the mid-plane.

Focussing on  $K_{ttop}$  (Fig.7a and Fig.7c), the opening values at the surface increase gradually with the simulated plastic wake length, following the trend observed in the bi-dimensional analysis at plane stress state. This behaviour is parallel at planes close to the surface, but the increment becomes smaller as we move into the specimen. When a certain plane is reached (approximately at  $z=1$  mm) this dependency vanishes and the results are basically constant.

At the mid-plane, the trend is slightly inverted, the opening values shown a small decrease with the plastic wake length. This trend is different from the observed in the previous bi-dimensional analysis at plane strain. However, the fact that the values at plane strain stabilise with less plastic wake than at the plane stress state remains the same. The same behaviour can be observed when the node contact criteria is analysed, as can be seen in Fig.7b and Fig.7d. The results obtained for closure, shows the same behaviour for the node contact criterion as can be seen in Fig.5c and Fig.5g. The exception is the tip tension criterion, where the behaviour is almost constant for all the plastic wake lengths considered.

#### 4. Plastic zone and contact area

Results corresponding to the plastic zone yielded with the different wake lengths and the contact patterns will be shown in this section. The observation of the evolution of this parameter in terms of the plastic wake provides a better comprehension about how the presence of the wake influences crack closure.

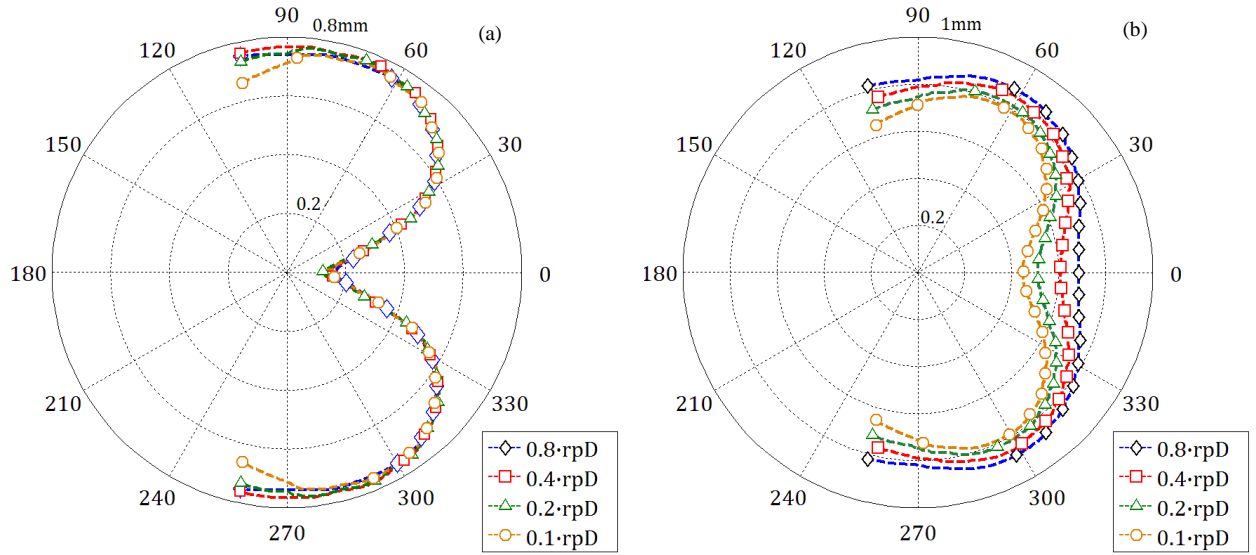


**Fig. 8.** Influence of the plastic wake length on the yielded area. (a) at the surface (b) at the mid-plane

Fig.8a and Fig.8b present the yielded area at the surface and at the mid-plane, respectively. In these figures, the yielded areas ahead of the crack front are plotted for  $R=0.1$ . The crack front is located at the pole of the polar coordinate system. The whole plastic wake is not represented. Just a small part of the yielded area behind the crack front is plotted.

In these figures, it is interesting to observe that the yielded area at the surface is not affected by the plastic wake length simulated, while the yielded area at the mid-plane changes slightly. The longer the plastic wake simulated, the greater the yielded area. In particular, the plane in which the yielded area changes the most is the fracture plane.

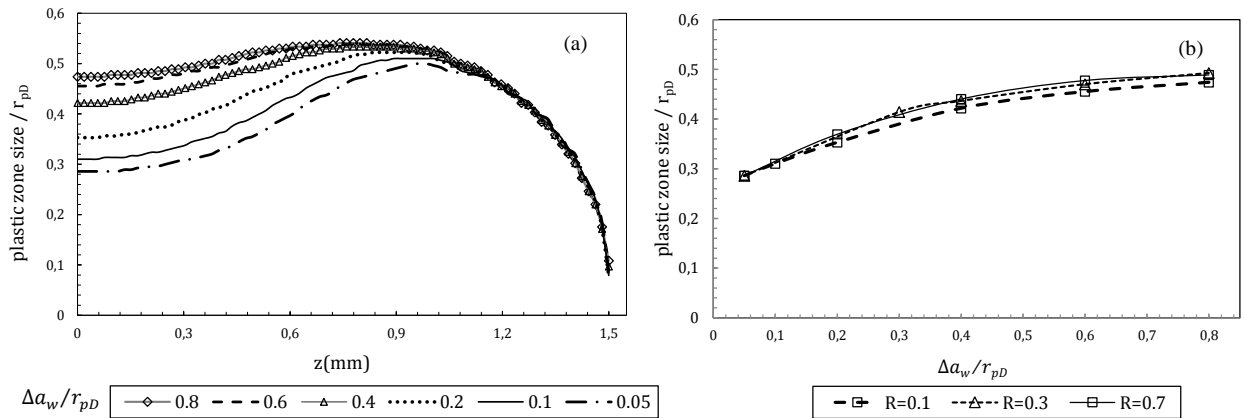


**Figure 9.** Influence of the plastic wake length on the plastic zone size at the fracture surface. (a) Yielded area at the fracture surface with  $R=0.1$ . (b) Plastic zone size at the mid-plane for  $R=0.1, 0.3$  and  $0.7$ .

Fig.9a shows the evolution of the yielded area at the fracture surface with the plastic wake length for  $R=0.1$ . In these figures can be clearly seen that the plastic wake length simulated has a huge influence in the yielded area at the bulk of the material from a certain distance from the surface, while close to the surface, the effect of the simulated plastic wake length is negligible. In particular, the yielded area ahead of the crack front at the mid-plane ( $z=0$ ) considering a plastic wake length equal to  $0.8 \cdot r_{pD}$  is about a 36% greater than the yielded area when the plastic wake length is  $0.05 \cdot r_{pD}$ , while at the surface ( $z=1.5\text{mm}$ ), the difference is less than 2%.

The extension of the plastic zone at the mid-plane is plotted in Fig.9b in terms of the plastic wake for the different values of  $R$ . It can be observed how the evolution of the plastic wake is independent of  $R$  and moreover, it can be concluded that the extension of the plastic zone has no influence over crack closure.

This analysis can be completed with the evaluation of the change of the contact pattern of the crack when the wake is developing. Fig.10a and Fig.10b present the contact areas obtained for the  $R=0.1$  and  $R=0.3$  cases, respectively. The  $R=0.7$  case is not represented because there are no contact points at the fracture surface. In general terms, it can be observed the expected contact pattern displaced towards the external face of the specimen. Nevertheless, differences may be found as the plastic wake develops.

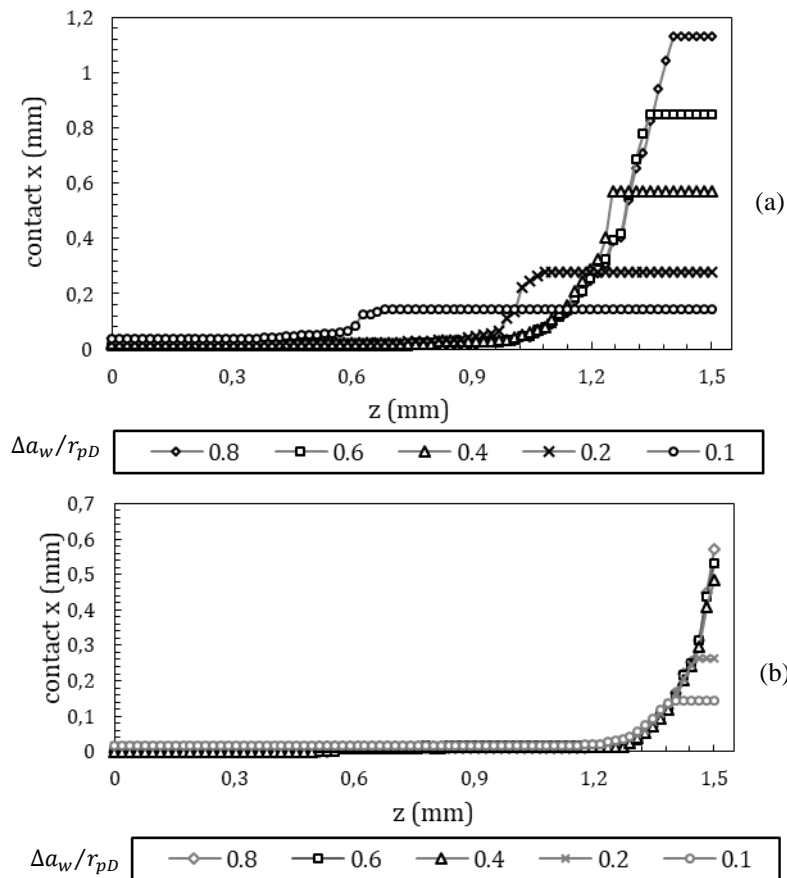


**Fig. 10.** Evolution of the contact areas with the plastic wake length (a)  $R=0.1$  (b)  $R=0.3$

Analysing Fig.10a, it can be seen that the maximum plastic wake length simulated ( $\Delta a_w = 0.8 \cdot r_{pD}$ ) is not enough to completely develop the whole contact area, a sharp cut can be observed. However, the trend is clear and can be easily deduced by extrapolation. Longer plastic wake just simply will extend the contact zone, but the pattern along the thickness is already defined. In fact, with the  $0.6 \cdot r_{pD}$  plastic wake length this shape is reached. For lower values, the contact area extends toward the interior and can be considered that the plastic wake simulated is not enough to represent the problem.

Nevertheless, it is somehow contradictory that opening and closure values (shown in previous section) are not affected for this circumstance. Even when the node contact criterion is used. This suggests that crack opening is dominated by the strain and stress field at a zone very close to the crack tip instead of the contact area (or the plastic zone previously seen).

Fig.10b, corresponds to the  $R=0.3$  case, where it can be observed that the contact surfaces are completely developed for the  $0.4 \cdot r_{pD}$  plastic wake length cases. In these cases, it should be enough to simulate a plastic wake of this value or even shorter, because the trend of the values along the thickness is clear and the rest of the curve could be easily deduced. Again there is a difference between the plastic wake necessary to stabilize the contact area and those needed to obtain opening and closure values.

One of the interesting conclusion of this analysis is that these parameters (yielded area and contact) need more wake to be simulated to consider that they are steady values, meanwhile crack closure need lower crack extensions. This means that opening and closure values are not directly influenced by these parameters, they are more dependent on the stress and strain field in a local area around the crack front which stabilised more quickly that the other global parameter which takes more cycles.

## 5. CONCLUSIONS

The study made in the present paper sets out the influence of the plastic wake length on different results under three-dimensional numerical simulations. It has shown the relevance that this parameter has on the crack opening and closure values, on the yielded areas on the interior of the specimen and on the contact surfaces along the thickness.

The results of this analysis indicate that at least a  $0.6 \cdot r_{pD}$  plastic wake length is necessary to develop in order to stabilise the main results. As this plastic wake length can be calculated in an allowable amount of time, it has been considered for the analysis under fatigue loading conditions.

Nevertheless, a reduced plastic wake length could be acceptable to obtain proper values in terms of crack opening or closure results, even when the plastic zone or the contact area was not completely defined. A plastic wake extension of  $0.2 \cdot r_{pD}$  for  $R=0.1$  and  $0.1 \cdot r_{pD}$  for  $R=0.3$  and  $R=0.7$  would be acceptable given the high computational cost of these calculation.

It also has been shown that the opening values when considering the stresses and displacements based criteria are really similar, while the behaviour on closure are completely different. During the unloading,

1 the stresses pass quickly to compression while physical closure of the flanks needs a little extra  
2 unloading.

3 Finally, this study indicates that the plastic wake length necessary to stabilise the main results as plastic  
4 zone or contact area is longer than those needed to obtain proper values in terms of crack opening or  
5 closure results. This suggests some independence among this parameter and fatigue crack closure.  
6  
7

### 8 **Acknowledgment**

9  
10 This work has been supported by the Ministerio de Economía y Competitividad of the Spanish  
11 Government through grant reference MAT2016-76951-C2-2-P.  
12

### 13 **References**

- 14 [1] Elber W. Fatigue crack closure under cyclic tension. *Eng Fract Mech* 1970;2:37–45.  
15  
16 [2] Suresh S, Ritchie RO. On the influence of fatigue underloads on cyclic crack growth at low stress  
17 intensities. *Mater Sci Eng* 1981;51:61–9. doi:10.1016/0025-5416(81)90107-5.  
18  
19 [3] Rao KTV, Yu W, Ritchie RO. On the behavior of small fatigue cracks in commercial aluminum-  
20 lithium alloys. *Eng Fract Mech* 1988;31:623–35. doi:10.1016/0013-7944(88)90105-1.  
21  
22 [4] Ashbaugh NE. Effects of load history and specimen geometry on fatigue crack closure  
23 measurements. *Mech Fatigue Crack Closure, ASTM STP 982* 1988:186–96.  
24  
25 [5] Ray SK, Grandt AF. Comparison of methods for measuring fatigue crack closure in a thick  
26 specimen. In: J.C. Newman J, Elber W, editors. *Mech. fatigue Crack Closure, ASTM STP 982*,  
27 Philadelphia: American Society for Testing and Material; 1988, p. 197–213.  
28  
29 [6] Yisheng W, Schijve J. Fatigue crack closure measurement on 2024-T3 sheet specimens. *Fatigue*  
30 *Fract Eng Mater Struct* 1995;18:917–21.  
31  
32 [7] Yoneyama S, Ogawa T, Kobayashi Y. Evaluating mixed-mode stress intensity factors from full-  
33 field displacement fields obtained by optical methods. *Eng Fract Mech* 2007;74:1399–412.  
34 doi:10.1016/j.engfracmech.2006.08.004.  
35  
36 [8] Vasco-Olmo JM, James MN, Christopher CJ, Patterson EA, Díaz FA. Assessment of crack tip  
37 plastic zone size and shape and its influence on crack tip shielding. *Fatigue Fract Eng Mater*  
38 *Struct* 2016;39. doi:10.1111/ffe.12436.  
39  
40 [9] Yusof F, Lopez-Crespo P, Withers PJ. Effect of overload on crack closure in thick and thin  
41 specimens via digital image correlation. *Int J Fatigue* 2013;56:17–24.  
42  
43  
44  
45  
46  
47  
48  
49  
50  
51  
52  
53  
54  
55  
56  
57  
58  
59  
60  
61  
62  
63  
64  
65

- 1  
2  
3  
4  
5  
6  
7  
8  
9  
10  
11  
12  
13  
14  
15  
16  
17  
18  
19  
20  
21  
22  
23  
24  
25  
26  
27  
28  
29  
30  
31  
32  
33  
34  
35  
36  
37  
38  
39  
40  
41  
42  
43  
44  
45  
46  
47  
48  
49  
50  
51  
52  
53  
54  
55  
56  
57  
58  
59  
60  
61  
62  
63  
64  
65
- [10] Camas D, Garcia-Manrique J, Gonzalez-Herrera A. Three-dimensional effects in the fracture mechanics of bi-dimensional specimens. 2012.
  - [11] González-Herrera A, Zapatero J. Influence of minimum element size to determine crack closure stress by the finite element method. *Eng Fract Mech* 2005;72:337–55. doi:10.1016/j.engfracmech.2004.04.002.
  - [12] Zapatero J, Moreno B, González-Herrera A. Fatigue crack closure determination by means of finite element analysis. *Eng Fract Mech* 2008;75:41–57. doi:10.1016/j.engfracmech.2007.02.020.
  - [13] Camas D, Hiraldo I, Lopez-Crespo P, Gonzalez-Herrera A. Numerical and experimental study of mixed-mode cracks in non-uniform stress field. *Procedia Eng.*, vol. 10, 2011, p. 1691–6.
  - [14] Camas D, Garcia-Manrique J, Gonzalez-Herrera A. Crack front curvature: Influence and effects on the crack tip fields in bi-dimensional specimens. *Int J Fatigue* 2012;44:41–50. doi:10.1016/j.ijfatigue.2012.05.012.
  - [15] Garcia-Manrique J, Camas D, Lopez-Crespo P, Gonzalez-Herrera A. Stress intensity factor analysis of through thickness effects. *Int J Fatigue* 2013;46:58–66. doi:10.1016/j.ijfatigue.2011.12.012.
  - [16] Garcia-Manrique J, Camas D, Gonzalez-Herrera A. Study of the stress intensity factor analysis through thickness: methodological aspects. *Fatigue Fract Eng Mater Struct* 2017;40:1295–308. doi:10.1111/ffe.12574.
  - [17] Garcia-Manrique J, Camas D, Parrón-Rubio ME, Gonzalez-Herrera A. Corrections in numerical methodology to evaluate plasticity induced crack closure along the thickness. *Theor Appl Fract Mech* 2018;97:215–23. doi:10.1016/j.tafmec.2018.08.004.
  - [18] Garcia-Manrique J, Camas-Peña D, Lopez-Martinez J, Gonzalez-Herrera A. Analysis of the stress intensity factor along the thickness: The concept of pivot node on straight crack fronts. *Fatigue Fract Eng Mater Struct* 2018;41. doi:10.1111/ffe.12734.
  - [19] Gonzalez-Herrera A, Zapatero J. Numerical study of the effect of plastic wake on plasticity-induced fatigue crack closure. *Fatigue Fract Eng Mater Struct* 2009;32:249–60. doi:10.1111/j.1460-2695.2009.01335.x.
  - [20] Alizadeh H, Hills DA, de Matos PFP, Nowell D, Pavier MJ, Paynter RJ, et al. A comparison of

two and three-dimensional analyses of fatigue crack closure. *Int J Fatigue* 2007;29:222–31.

doi:10.1016/j.ijfatigue.2006.03.014.

- [21] Gardin C, Fiordalisi S, Sarrazin-Baudoux C, Gueguen M, Petit J. Numerical prediction of crack front shape during fatigue propagation considering plasticity-induced crack closure. *Int J Fatigue* 2016;88:68–77. doi:10.1016/j.ijfatigue.2016.03.018.
- [22] Gardin C, Fiordalisi S, Sarrazin-Baudoux C, Petit J. Numerical simulation of fatigue plasticity-induced crack closure for through cracks with curved fronts. *Eng Fract Mech* 2016;160:213–25. doi:10.1016/j.engfracmech.2015.11.023.
- [23] Vor K, Gardin C, Sarrazin-Baudoux C, Petit J. Wake length and loading history effects on crack closure of through-thickness long and short cracks in 304L: Part II - 3D numerical simulation. *Eng Fract Mech* 2013;99. doi:10.1016/j.engfracmech.2013.01.014.
- [24] Antunes F V, Correia L, Camas D, Branco R. Effect of compressive loads on plasticity induced crack closure. *Theor Appl Fract Mech* 2015;80:193–204. doi:10.1016/j.tafmec.2015.09.001.
- [25] Borrego LP, Antunes FV, Costa JD, Ferreira JM. Numerical simulation of plasticity induced crack closure under overloads and high–low blocks. *Eng Fract Mech* 2012;95:57–71. doi:10.1016/j.engfracmech.2012.07.016.
- [26] Camas D, Garcia-Manrique J, Moreno B, Gonzalez-Herrera A. Numerical modelling of three-dimensional fatigue crack closure: mesh refinement. *Int J Fatigue* 2018. doi:10.1016/j.ijfatigue.2018.03.035.
- [27] Camas D, Garcia-Manrique J, Gonzalez-Herrera A. Numerical study of the thickness transition in bi-dimensional specimen cracks. *Int J Fatigue* 2011;33:921–8. doi:10.1016/j.ijfatigue.2011.02.006.
- [28] Camas D, Lopez-Crespo P, Gonzalez-Herrera A, Moreno B. Numerical and experimental study of the plastic zone in cracked specimens. *Eng Fract Mech* *Accept Publ* 2017.
- [29] Fleck NA. Finite element analysis of plasticity-induced crack closure under plane strain conditions. *Eng Fract Mech* 1986;25:441–9.
- [30] Solanki K, Daniewicz SRR, Newman JCC. A new methodology for computing crack opening values from finite element analyses. *Eng Fract Mech* 2004;71:1165–75. doi:10.1016/S0013-

7944(03)00113-9.

- 1  
2 [31] Wei L-W, James MN. A study of fatigue crack closure in polycarbonate CT specimens. Eng Fract  
3 Mech 2000;66:223–42. doi:DOI: 10.1016/S0013-7944(00)00014-X.  
4  
5  
6 [32] McClung RC, Sehitoglu H. On the finite element analysis of fatigue crack closure-1. Basic  
7 modeling issues. Eng Fract Mech 1989;33:237–52.  
8  
9  
10 [33] de Matos PFP, Nowell D. Numerical simulation of plasticity-induced fatigue crack closure with  
11 emphasis on the crack growth scheme: 2D and 3D analyses. Eng Fract Mech 2008;75:2087–114.  
12 doi:10.1016/j.engfracmech.2007.10.017.  
13  
14  
15 [34] Antunes F V, Rodrigues DM. Numerical simulation of plasticity induced crack closure:  
16 Identification and discussion of parameters. Eng Fract Mech 2008;75:3101–20.  
17 doi:10.1016/j.engfracmech.2007.12.009.  
18  
19  
20  
21  
22  
23  
24  
25  
26  
27  
28  
29  
30  
31  
32  
33  
34  
35  
36  
37  
38  
39  
40  
41  
42  
43  
44  
45  
46  
47  
48  
49  
50  
51  
52  
53  
54  
55  
56  
57  
58  
59  
60  
61  
62  
63  
64  
65